A New Method to Analyze the Tsunami Incitement Process and Site-selection for Tsunami Observations in China's Eastern Sea

Yuanqing Zhu[1],
Shuangqing Liu,
Yanlin Wen,
Yan Xue

[1]*Professor, Earthquake Administration of Shanghai Municipality;*
National Geophysical Observatory at Sheshan, Shanghai, 200062, China
Email: yqzhu@sbsn.net, liushuangq05@mails.gucas.ac.cn

ABSTRACT

In this paper, we present a CONTROL volume model for tsunami incitement process by combining the Navier-Stokes equation, the jet theory and relative velocity model. We conclude that the initial condition for tsunami propagation simulation is equivalent to the static near-field seismic displacement of earthquake that induces the tsunami. The error analyzed from this method is only about 1 percent for a common seafloor earthquake, and it is consistent with the result of Ansys/Ls-dyna numerical analysis. EDGRN/EDCMP and COMCOT program provide some new acquirement for the tsunami studies. In the second part of the paper, we develop a site-selection method for anchor-grounded tsunami observation in Chinese eastern sea.

KEYWORDS: N-S equation, Jet theory, Relative velocity, Optimal analysis

INTRODUCTION

At present, there is little solid and constructive study on the tsunami near-field characteristics or initial condition of propagating simulation. The classic paper by Gutenberg (1939) showed that most previous studies on tsunami were rested on the qualitative approaches. The essential study about the tsunami near-field characteristics maybe owned to Kajiura (1970). He separated the energy pattern from the non-homogeneous wave equation. Most of subsequent tsunami propagation researches all made a statement to cite its conclusion, albeit there was a defect in that article, which the energy of dynamic retrieved from the incitement source was completely independent of the water depth. Based on the linear shallow water wave equations, Todorovska et al. (2001,2002,2003) derived analytical integral solution for tsunami incited by a landslide. Ward (2003) deduced, with traditional seismological procedures, some 1st-order approximate integral formula of results including patterns of incitement of the landslide, celestial impact, and seismic tensor combined with focal geometry parameters. Ohmachi et al. (2001) utilized BEM and FDM methods to simulate a tsunami incitement process by a fault rupture. Partial interrelated experiments and corresponding numerical calculations were carried out by Grilli et al. (2001,2004,2005) and Liu et al. (2005). Except above, most researches put focus on the propagation and simulation algorithm, and paid little attention to the "initial value problem." We present a new way to analyze the tsunami near-field characteristics. Also, in the part 2, we discuss the method for selecting a best site for anchor-grounded tsunami observational station.

PART (I) INITIAL VALUE PROBLEM

Mathematical Model

In general fluid mechanism theory, the Navier-Stokes momentum equation is

$$\frac{\partial \boldsymbol{V}}{\partial t} + \boldsymbol{V}\cdot\nabla\boldsymbol{V} = \boldsymbol{f} + \frac{1}{\rho}\nabla\cdot(T_{ij}\boldsymbol{e}_i\boldsymbol{e}_j) \tag{1}$$

Where, $\boldsymbol{V}$ is velocity vector, $\boldsymbol{f}$ is body force, $\boldsymbol{\rho}$ is density, T_{ij} is a tenor, and $\boldsymbol{e}_i$, $\boldsymbol{e}_j$ is unit directional vector. This is a differential equation. Along with the continuous equation: $\frac{\partial \rho}{\partial t} + \nabla\cdot(\rho\boldsymbol{V}) = 0$, it constitutes the traditional foundation of fluid mechanism theory. Especially, they are suitable for the shallow wave studies. However, these equations only allow researchers to derive the complex integral solutions to the wave initial deformation, it is still difficult to obtain the relationship between the tsunami and its incitement source, even for the case in which the hypothesis source is very simple. But if we consider the integral equation form of momentum is

$$\int_D \frac{\partial(\rho\boldsymbol{V})}{\partial t}d\mathrm{V} + \oiint_{\Sigma}\rho\boldsymbol{V}(\boldsymbol{V}\cdot\boldsymbol{n})dA = \int_D \rho\boldsymbol{f}d\mathrm{V} + \oiint_{\Sigma}\boldsymbol{T}_n dA \tag{2}$$

Where $\boldsymbol{n}$ is a normal vector. We can develop a CONTROL volume model to analyze it.

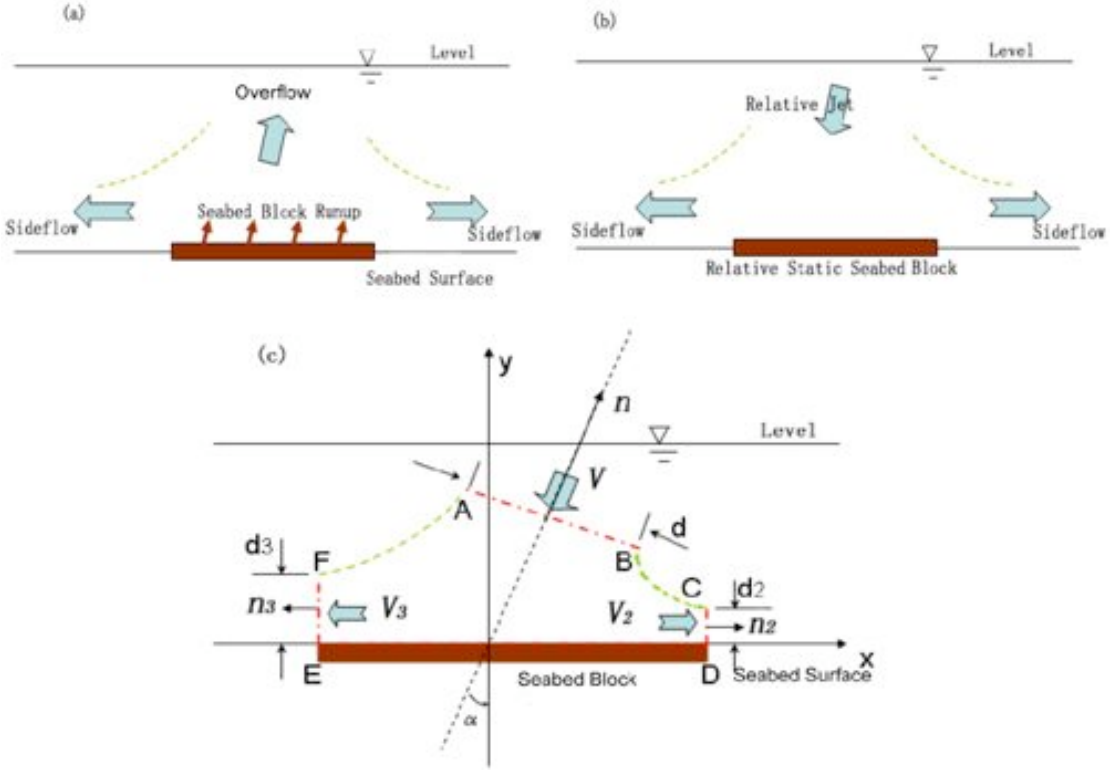

Fig .1 The sketch of two-dimensional sea disturbance by seabed run-up
(a) Incitement of seabed run up, (b) The model of jet on the approach of relative velocity analysis,
(c) The Cartesian-ordinates description of steady jet model and CONTROL volume.

When a seafloor earthquake takes place, the nearby seabed would lift up and pull down, the water column above the seabed would be disturbed and tsunami could possibly be generated. We simplify the tsunami incitement process as the Fig.1 and only consider the seabed lift-up case. We assume that the sea bed lifts up with a constant velocity until the earthquake rise time ends. The sea water is uplifted with slower velocity $\boldsymbol{V}_1$ than that of sea bed $\boldsymbol{V}_0$. We then define the relative velocity $\boldsymbol{V}=\boldsymbol{V}_1-\boldsymbol{V}_0$, and the overflow can take as a relative jet flow with velocity $\boldsymbol{V}$ (see the fig. 1(b)). It can be farther modified as the CONTROL volume model in the fig. 1(c), in which $\boldsymbol{V}_2$ and $\boldsymbol{V}_3$ represent the velocities of two right-about side flows respectively.

The region closed by AB-BC-CD-DE-EF-FA (figure 1c) is the CONTROL volume. The reference frame is x-axis trends along the sea bed, y-axis goes up, and z-axis is a unit length. The jet flow, with a width **d**, impacts the sea bed with an angle of incidence $\boldsymbol{\acute{a}}$. In the specified CONTROL volume, we assume the body force $\boldsymbol{f}$ is zero and the flow is uncompressible, the equation (2) can be rewritten as

$$\oiint_{\Sigma}\rho\boldsymbol{V}(\boldsymbol{V}\cdot\boldsymbol{n})dA=-\oiint_{\Sigma}p\boldsymbol{n}dA \tag{3}$$

and

$$\oiint_{\Sigma}\rho\boldsymbol{V}(\boldsymbol{V}\cdot\boldsymbol{n})dA=\iint_{AB}\rho\boldsymbol{V}(\boldsymbol{V}\cdot\boldsymbol{n})dA+\iint_{BC+FA}\rho\boldsymbol{V}(\boldsymbol{V}\cdot\boldsymbol{n})dA+\iint_{CD}\rho\boldsymbol{V}_2(\boldsymbol{V}_2\cdot\boldsymbol{n})dA+\iint_{EF}\rho\boldsymbol{V}_3(\boldsymbol{V}_3\cdot\boldsymbol{n})dA \tag{4}$$

In equation (4), $\boldsymbol{V}\cdot\boldsymbol{n}=0$ on the BC+FA boundary, because they are the jet flow side and the normal velocity equals zero. Therefore, we have

$$\begin{aligned}\oiint_{\Sigma}\rho\boldsymbol{V}(\boldsymbol{V}\cdot\boldsymbol{n})dA&=-\rho\boldsymbol{V}Vd+\rho V_2^2d_2\boldsymbol{i}-\rho V_3^2d_3\boldsymbol{i}\\&=-\rho V^2d(\boldsymbol{i}\sin\alpha+\boldsymbol{j}\cos\alpha)+\rho V_2^2d_2\boldsymbol{i}-\rho V_3^2d_3\boldsymbol{i}\end{aligned} \tag{5}$$

Where V_2, V_3 are unbeknown parameters. Making use of the steady Bernoulli formula

$$p_a+\frac{\rho V^2}{2}=p_a+\frac{\rho V_2^2}{2}=p_a+\frac{\rho V_3^2}{2} \tag{6}$$

Where, p_a is the environmental pressure. We deduce the result of $V=V_2=V_3$. Furthermore, $Vd=V_2d_2+V_3d_3=V(d_2+d_3)$ by analysis of continuous equation, and $d=d_2+d_3$ subsequently.

Now we calculate the sum of pressure with

$$-\oiint p\boldsymbol{n}dA=-\iint_{AB+BC+CD+EF+FA}p_a\boldsymbol{n}dA-\iint_{DE}p\boldsymbol{n}dA \tag{7}$$

$-\iint_{DE}p\boldsymbol{n}dA$ represents the force that the seabed acts on the water. Given the pressure of the down-toward side of sea bed is p_{struc}, the sum of force on the sea bed (ED length) is

$$\boldsymbol{F}=\iint_{DE}(p-p_{struc})\boldsymbol{n}dA \tag{8}$$

Substitute p into equation (7), we have

$$\begin{aligned} \boldsymbol{F} &= \iint_{DE}(p - p_{struc})\boldsymbol{n}dA = \oiint p\boldsymbol{n}dA - \iint_{AB+BC+CD+EF+FA} p_a\boldsymbol{n}dA - \iint_{DE} p_{struc}\boldsymbol{n}dA + \iint_{DE} p_a\boldsymbol{n}dA - \iint_{DE} p_a\boldsymbol{n}dA \\ &= \oiint p\boldsymbol{n}dA - \oiint p_a\boldsymbol{n}dA - \iint_{DE} p_{struc}\boldsymbol{n}dA + \iint_{DE} p_a\boldsymbol{n}dA \end{aligned} \tag{9}$$

The second item on the right is equal to zero as it integrates on a closed facet. And equation (9) can be simplified as

$$\boldsymbol{F} = \oiint p\boldsymbol{n}dA - \iint_{DE} p_{struc}\boldsymbol{n}dA + \iint_{DE} p_a\boldsymbol{n}dA \tag{10}$$

Substitute equations (10), (5) into (3):

$$-\rho V^2 d(\boldsymbol{i}\sin\alpha + \boldsymbol{j}\cos\alpha) + \rho V^2 d_2\boldsymbol{i} - \rho V^2 d_3\boldsymbol{i} = -\boldsymbol{F} - \iint_{DE} p_{struc}\boldsymbol{n}dA + \iint_{DE} p_a\boldsymbol{n}dA$$

then

$$\begin{aligned} \boldsymbol{F} &= \rho V^2 d(\boldsymbol{i}\sin\alpha + \boldsymbol{j}\cos\alpha) - \rho V^2 d_2\boldsymbol{i} + \rho V^2 d_3\boldsymbol{i} - \iint_{DE} p_{struc}\boldsymbol{n}dA + \iint_{DE} p_a\boldsymbol{n}dA \\ &= -\iint_{DE} p_{struc}\boldsymbol{n}dA + \iint_{DE} p_a\boldsymbol{n}dA + (\rho V^2 d\cos\alpha)\boldsymbol{j} - (\rho V^2 d_2 - \rho V^2 d_3 - \rho V^2 d\sin\alpha)\boldsymbol{i} \end{aligned} \tag{11}$$

Considering the water is approximately an idealized fluid, only the normal force exists on the seabed, and the x-axis component of $\boldsymbol{F}$ is zero.

$$\boldsymbol{F} = -\iint_{DE} p_{struc}\boldsymbol{n}dA + \iint_{DE} p_a\boldsymbol{n}dA + (\rho V^2 d\cos\alpha)\boldsymbol{j} \tag{12}$$

$$d_2 - d_3 = d\sin\alpha \tag{13}$$

Since $d_2 + d_3 = d$, we have $d_2 = \dfrac{d(1+\sin\alpha)}{2}$ and $d_3 = \dfrac{d(1-\sin\alpha)}{2}$.

Hereby, the inter-force on the interface between water and sea bed can be written as

$$\boldsymbol{F}_{\text{int}eraction} = (-\rho V^2 d\cos\alpha)\boldsymbol{j} - \iint_{DE} p_a\boldsymbol{n}dA \tag{14}$$

Therefore, $\boldsymbol{F}_{\text{interaction}}$ is a function of the fluid density, relative velocity and incidence angle of jet, the pressure of environment, and the ED length of seabed incitement. If we assume the length of ED is l, $d = \kappa l$, $\kappa \in (0,1)$ is a ratio (we define it as a factor of effective width of jet flow), then

$$\boldsymbol{F}_{\text{int}eraction} \approx (-\rho V^2 \kappa l\cos\alpha)\boldsymbol{j} - l\rho gh\cdot\boldsymbol{n}$$

$$\| F_{\text{int}eraction} \|_1 = \rho V^2 \kappa l\cos\alpha + l\rho gh = \rho l(\kappa V^2\cos\alpha + gh) \tag{15}$$

In fact, the value of κ reflects the homogenization of fluid velocity and pressure on the entrance and exit of jet. Where, g is the gravity acceleration force, h is the depth of water.

We can also consider the effect of $\boldsymbol{F}_{\text{interaction}}$ to the water energy by the formula $\frac{\partial E}{\partial t} = \oiint_{\Sigma} \boldsymbol{T}_n \cdot \boldsymbol{V} dA$, where E is the total energy of water.

$$\begin{aligned}\frac{\partial E}{\partial t} &= \oiint_{\Sigma} \boldsymbol{T}_n \cdot \boldsymbol{V} dA = \iint_{\Sigma} \boldsymbol{F}_{\text{int}eraction} \cdot \boldsymbol{V} dA = \iint_{\Sigma} ((-\rho V^2 \kappa l \cos\alpha)\boldsymbol{j} - l\rho g h \cdot \boldsymbol{n}) \cdot \boldsymbol{V} dA \\ &= \iint_{\Sigma} \rho V l(\kappa V^2 \cos^2\alpha + gh\cos\alpha) dA\end{aligned} \tag{16}$$

The above equation is very simple but with an important implication to separate the pattern of energy. We can define Q to illustrate the result as well:

$$Q = c \cdot V^2 / gh \tag{17}$$

Where, c is the ratio of $\kappa \cos^2\alpha$ and $\cos\alpha$ in the equation (16).

It is believed that, once a tsunami is induced by an earthquake, the uplift velocity of seabed is between 0.1-10m/s, and h is between 500-5000m. According to Equation (17), Q would be in the range of 2.04×10^{-7} to 0.0204 if c is about 1. This range of Q value shows that, compared with the potential energy, the kinetic energy of water is very small in the tsunami incitement process. On the other hand, the initial tsunami height is correlated with the energy of the potential; hence, we can conclude that tsunami propagation simulating initial condition is approximately replaced by the seismic static near-field displacement.

To test this statement, we did an Ansys/Ls-Dyna numerical simulation.

Ls-Dyna is mainly an explicit scheme code first developed by Hallquist (1976), and it became a commercial product inbuilt in the Ansys software around 2003. Anghileri et al. (2005) used it to simulate four descriptive patterns of water model. We utilize the Lagrange method to simulate the water. The model parameters are given in table 1.

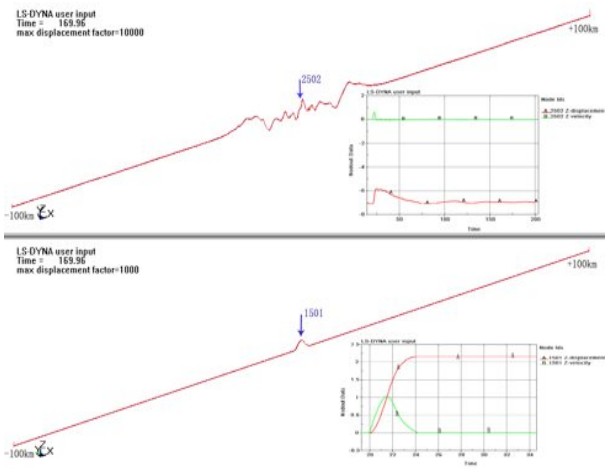

Fig.2 The sea level deformation after about 150s by the incitement and the evolution of velocity and displacement on node 1501(level) and node 2502(seabed)

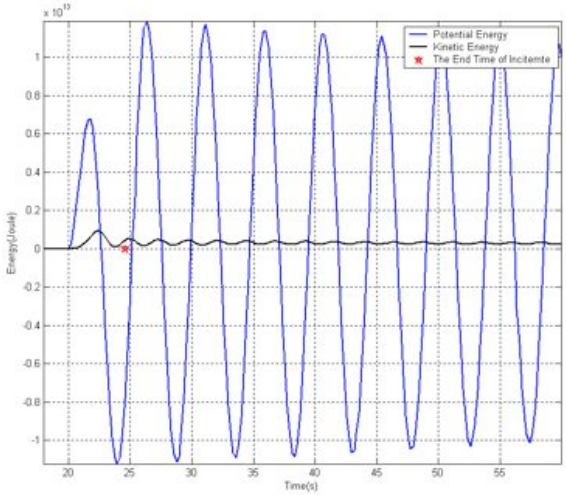

Fig.3 The evolution of potential and kinetic energy in the incitement progress, "★" the end time of incitement

Table 1 the parameters of water model

*MAT_NULL							
1	1000.0	0	0	0	0	0	0
*EOS_GRUNEISEN							
1	1.647E3	1.921	-0.096	0	0.350	0	0
0.0							

In the simulation, the depth of water, which considered to be the compressible GRUNEISEN model (see table 1), is 2000 meters. We establish a three dimensional calculation, but the y-axis is a "unit" length (200 meters, a length of lattice). A 5 km width sea bed with a smooth run-up sites in middle (see fig.2). As the compressibility of water, in the starting 20 seconds, we set the sea bed stationary; and a weight damping algorithm is engaged for creating an initial quasi-static sea environment. The evolution of potential and kinetic energy in the incitement progress is shown in Fig. 3. The difference of amplitude shows that the potential energy plays a dominant role. Fig.2 also shows that the disturbed water spreads with an approximate celerity of gravity water C ($C = \sqrt{gh}$). This result indicates that using the weight-damping algorithm in the calculation is very important; otherwise, like in the work of Ohmachi et al. (2005), the water wave spreads very fast; and we think their velocity is the sound speed in water instead of the tsunami prorogation's. As a result, static displacement is of satisfying approximation to initial tsunami wave, we can utilize the EDGRN/EDCMP program to calculate the effect of the dislocation, fault length, fault width, fault central depth, obliquity, and rake in the seismic near-field static displacement, in order to give the possibility of tsunami from different pattern of seafloor earthquakes (see the appendix).

PART (II) Determining the OPTIMAL ANCHOR-GROUNDED Tsunami OBSERVATIONAL STATION

In this section, we present a method to determine the best location for the anchor-grounded tsunami observation station in the region west of 126E. Three primary factors that control the site-selection include the clustered seismic activity, the population distribution of cities near China coastline and comparative propagation damping coefficient from the Manning formula.

The following factors are also taken into account:

(1) Seismic activity; there are 670 historical earthquake events, which span from 1976 to 2006 and spread across the 115-135 longitude and 20-41 latitude. The cluster method, K-means clustering, compress the 670 events into 40 representations.

(2) Altitude of each observation point; the land points (dry points) are set the weight of 3/8p, and p is an artificial small value for Surfer imaging. The total nodes in the model are 301□316(a node per 2 minute).

(3) National boundaries, namely, simply give a weight of 5/8p to the region east of 126^0 E.

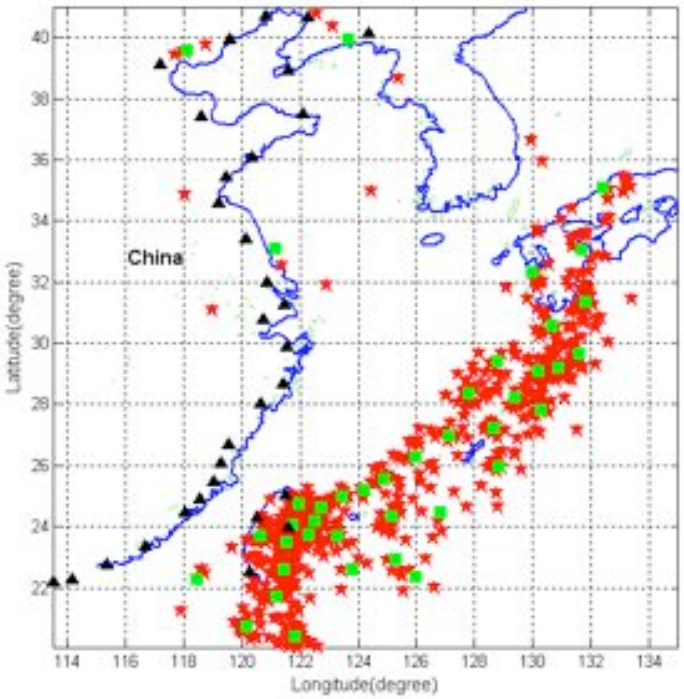

Fig. 4 The distribution of earthquake central (red star) in China eastern sea and neighboring region (1976-2006, Mw>5, data come from http://www.globalcmt.org/CMTsearch.html) and cluster central (green pane).

(4) Distance from the center of the nearest three cities **C**. If it is less than 50km, the weight is as small as *p*. The article includes 33 coastal cities, for instance, Macao, Hong Kong, Shanghai, Tianjin, Taipei, Taichung, Kaohsiung, Hualien and so on (see Fig. 4 the black triangle symbols).

The above four steps are engaged for reducing the cost of calculation.

(5) Synthesized effect of inshore cities. Here, we consider the systematical interaction among the observational station **R**, the nearest three cities population weighted position **C**, the sum population $Popu_k$ of three cities, and the angle θ between vector of **SR** and **RC** (see Fig. 6).

(6) Consumed time in the propagation of **SR**. The consumed time $\eta\_t = \dfrac{T\_mean}{T\_mean + T_{RS}}$, where, *T_mean* is that the span of calculation area divided by the mean of the gravity velocity of the total sea points, is modified by the *T_mean* in order to avoid the excess exaggeration of length effect of ray.

(7) Damping coefficient. Using the Manning formula $n = \sqrt{\dfrac{fh^{1/3}}{2g}}$, then $f = \dfrac{2n^2 g}{h^{1/3}}$ .And we define the $Q_{rs} = e^{-\varepsilon_1 \times L_{RS} \times \frac{(f_1 + f_2 + \cdots + f_k + \cdots + f_n)}{n}}$ for the whole damping effect for points of each propagation ray **RS**. ε_1 is a modulated factor. And the land points (dry points) are given a specified large friction (see Fig.5).

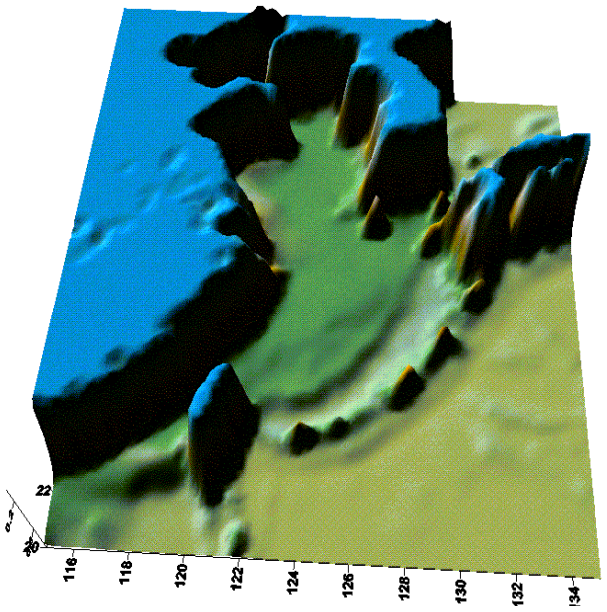

Fig. 5 Distribution of friction in the region

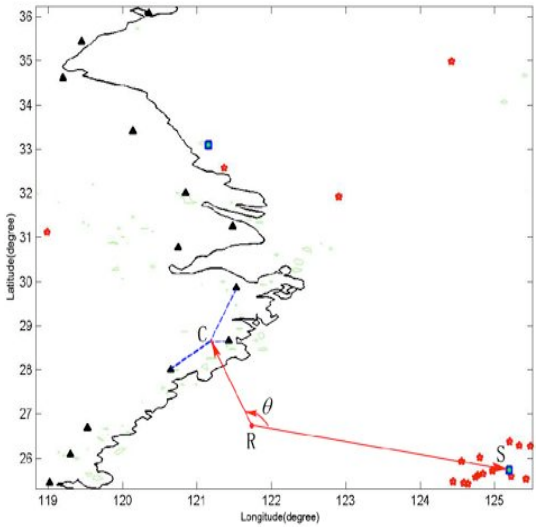

Fig. 6 The cluster central **S**, anchor point **R**, and the weighted central of cities **C**, and the angle $\boldsymbol{\theta}$

(8) Warning time and Cost; making use of $\mu(L) = v_i \times (\frac{1}{2L} + \frac{1}{0.28L + \frac{2000}{L-49}})$, ($L$≥50km) to replace the effect. $\mu(L)$ is approximately like the F-distribution of the Probability in the calculating interval. where, v_i is separated into three classes according to the water depth. In the article, let the ratio are 2:3:5 with respect to the 0-100, 100-600, 600-2000 meters.

(9) The ratio of land points in the ray **RS**; if the ratio is larger than 2/3, the effect of the j^{th} ray is set to be zero. The factor (9) can partly reflect the contributions of obstacle islands or land in collaboration with factor (7).

The mathematical model eventually is established as follow

$$P_i = \sum_k \{\mu(L_{R_i C_k}) \times Popu_k \times [\sum_j (Q_{R_i S_j} \times \eta\_t_{i,j} \times \sin(\frac{1}{2}\theta_{k,i,j})]\} \quad (18)$$

Calculation result is displayed in Fig. 7.

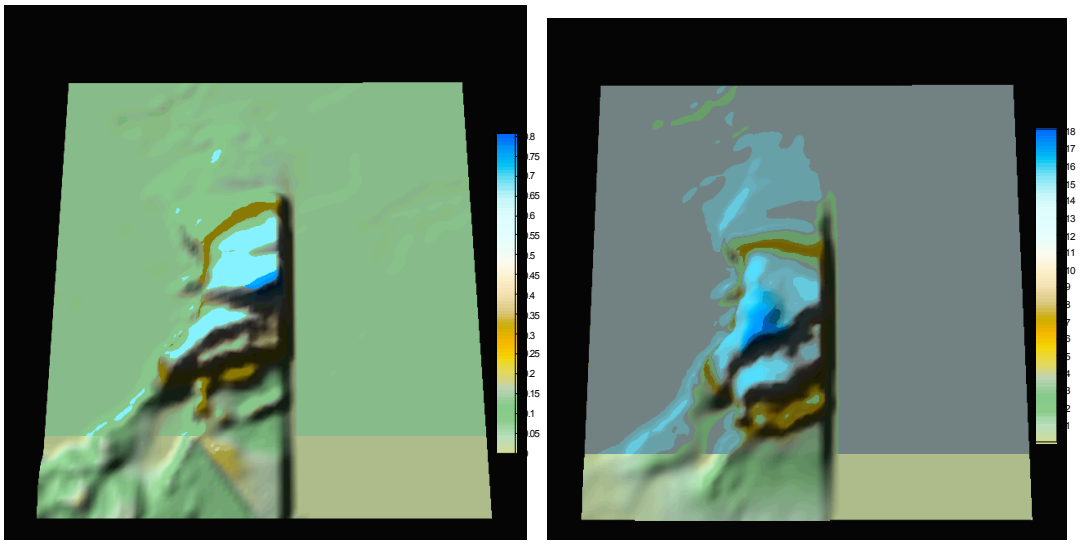

Fig.7 the weight of observational station anchor-grounded in Chinese eastern sea (color value only be compared in each picture respectively)
(a)Consider the 33 cities effect (b) Only concerned with Shanghai

According to the above result, we maybe take some action to decide how to emplace the observation station for tsunami precaution.

CONCLUSION

In this paper, we divide it into two parts. In the first part, we mainly discuss the interaction of fluid-structure in the tsunami incitement process. A valuable result is obtained that the tsunami initial height, which provided for propagation simulating condition, is closely the same as the seismic static near-field displacement. As this result, we can answer the comparative effects between different earthquake parameters by running the EDGRN/EDCMP program.

In the second part, we use the multiplicative principle to organize 9 factors to discuss the problem of observation station anchor-grounded for Chinese eastern sea region. Two cases of our calculations are displayed in Fig.7. They illustrate together an arc area with a high weight to the east of Zhejiang and Fujian provinces. The east-northern edge of Taiwan island get a much higher weight as well, but Bohai sea is a small weight area. It behooves us to make a reference for optimum of tsunami observation.

ACKNOWLEDGEMENTS

In the accomplishment of this paper, we have received the zealous help and support from Professor Steven, N.Ward, Dr. Yinchun Liu at University of Minnesota, USA, Dr. Rongjiang Wang, at Potsdam, Germany, and Dr. Ting Yang at Tongji University, Shanghai. We express our thanks for their generosity. The work is supported by the National Geophysical Observatory at Sheshan (2007FY220100), the Chinese Joint Seismological Science Foundation (106078) and NSFC (40576022).

APPENDIX

(I) *The Effect of Earthquake Parameters*

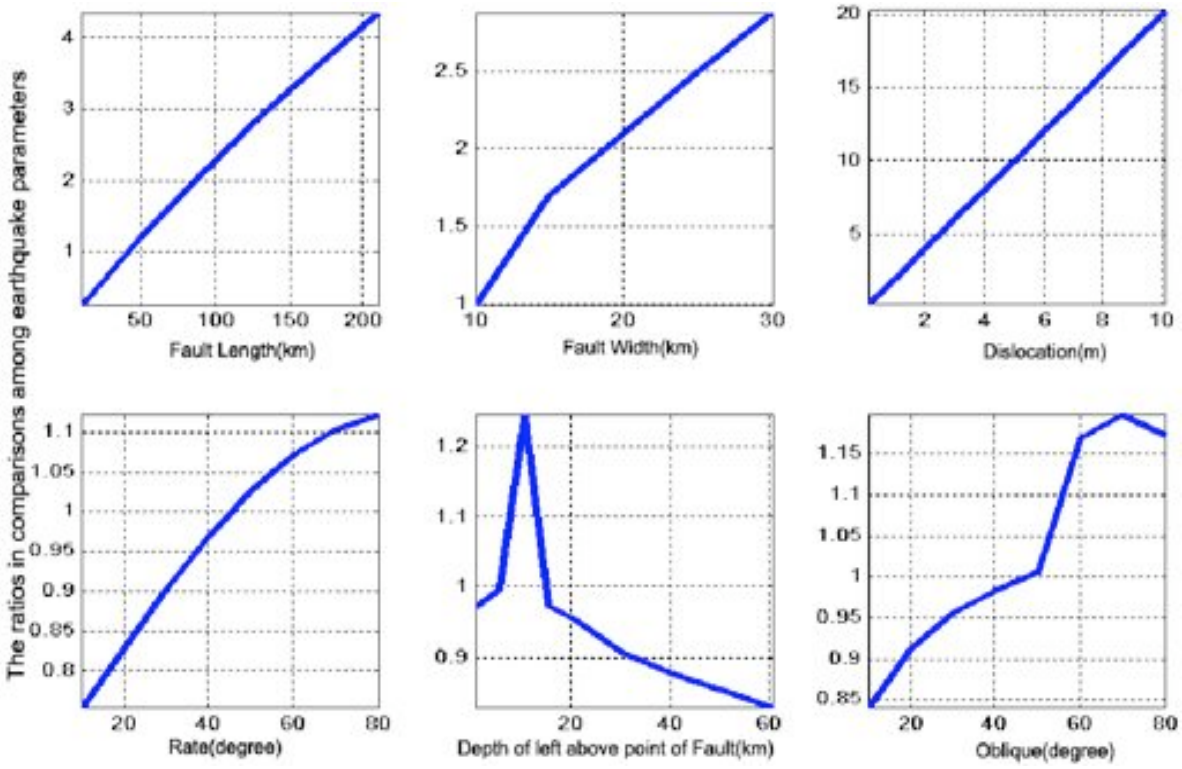

Fig. 8 The effect among different earthquake parameters

Fig.8 is calculated by the EDGRN/EDCMP program (Wang Rongjiang, 2003). As the expatiation in the Part (I), we conclude the tsunami initial propagation condition is closely the same as the seismic static near-field displacement. Usually, the tsunami is mainly disturbed by the vertical component of displacement, thus, we calculate a 400km×400km area deformation by diversified earthquakes, with 201×201nodes，then accumulate the absolute vertical displacement component on every node. Eliminating the disharmony between dimension of the calculating area and true disturbed area by earthquake, for instance, removing the case of the calculating area is less than true disturbed area, we make the each acuminated displacement component to be divided by a "unit" displacement by a referenced earthquake with a 40km fault length, 10km fault width, 5km depth of the left above fault point, 0.5m dislocation, 45^0 rate and 45^0 oblique. It is easy for us to discover that the dislocation plays the most important role in the near-field displacement, and there is an inflexion on the effect as the depth of epicenter becomes deeper gradually because of the effective energy released by earthquake.

(II) ***The Simulation Near the Yaeyama Islands***

Fig. 9 is a hypothetic tsunami nonlinear simulation near the Yaeyama islands, with the Manning constant n=0.012 and the COMCOT program (SCEE, 2006). The topography data of two minutes come from the NGDC. We interpret the data into the one-minute with a third-order B-spline method. The result indicates n=0.012 is credible for the actual calculating. Thus, in the part (II), we also set the n=0.012 for the factor (7).

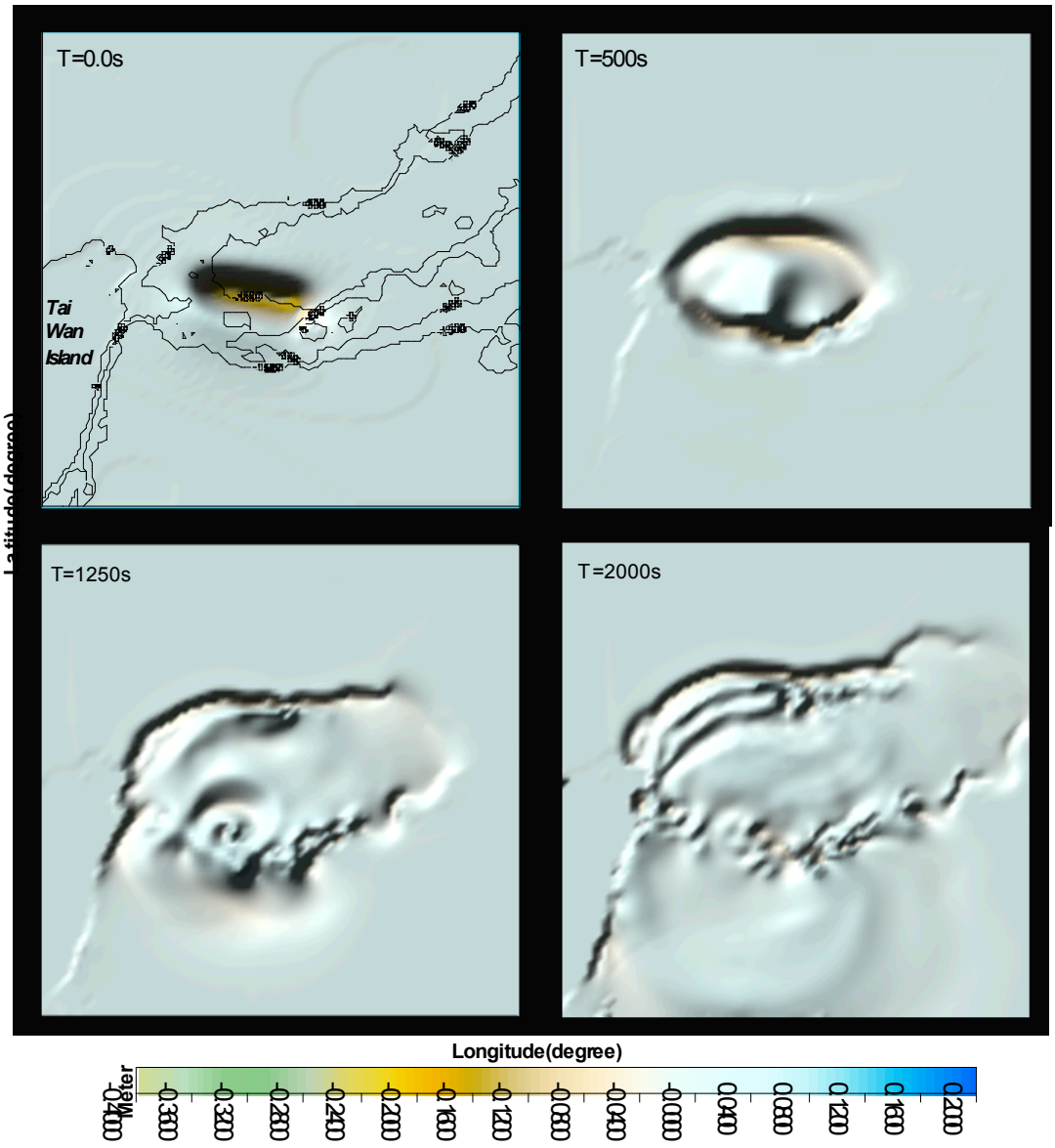

Fig. 9 A hypothesis tsunami simulation near the Yaeyama islands

REFERENCES

[1] Carlo Brandini, Stéphan T. Grilli.(2001). Modeling of freak wave generation in a 3D-NWT, To appear in Proc.ISOPE 2001 Conf. Stavanger, Norway (http://www.oce.uri.edu/~grilli/isope13.pdf)

[2] Gutenberg, B. (1939). Tsunamis and earthquakes, Bull, seism, Soc.America. **29:4**, 517-526

[3] John O.Hallquist (2006). LS-DYN A theory manual

[4] Kajiura, K (1970). Tsunami Source, Energy and the Directivity of Wave Radiation, Bulletin of the Earthquake Research Institute, **Vol.48**, 835-869

[5] M.D. Trifunac, A. Hayir, M.I. Todorovska. (2003). A note on tsunami caused by submarine slides and slumps spreading in one dimension with non-uniform displacement amplitudes, Soil Dynamics and Earthquake Engineering **Vol.23**, 223-234

[6] Maria I. Todorovska, Mihailo D. Trifunac (2001). Generation of tsunamis by a slowly spreading uplift of the sea floor, Soil Dynamics and Earthquake Engineering **Vol.21**, 151-167

[7] M.I.Todorovska, A.Hayir, M.D.Trifunac (2002). A note on tsunami amplitudes above submarine slides and slumps, Soil Dynamics and Earthquake Engineering **Vol.22**, 129-141

[8] Philip Watts, Stephan T. Grilli, M. Asce (2005). David R. Tappin and Gerard J.Fryer, Tsunami Generation by Submarine Mass Failure II: Predictive Equations and Case Studies, Journal of Waterway, Port, Coastal, and Ocean Engineering, **Vol.131, No.6**, November 1

[9] P.L.-F Liu, T. -R. Wu, F. Raichlen et al. (2005). Run-up and rundown generated by three-dimensional sliding masses, J. Fluid. Mech, 107-144

[10] Rongjiang Wang et al. (2003). Computation of deformation induced by earthquakes in a multi-layered elastic crust—FORTRAN programs EDGRN/EDCMP, Computers & Geosciences **Vol.29** (2003), 195-207

[11] SCEE (School of Civil and Environmental Engineering, Cornell University)(2006). COMCOT User Manual, Version 1.6

[12] Stéphan T. Grilli, Richard W. Gilbert (2004). Pierre Lubin et al., Numerical Modeling and Experiments for Solitary Wave Shoaling and Breaking over a Sloping Beach, Proceedings of The Thirteenth (2004) International Offshore and Polar Engineering Conference Toulon, France, May23-28, 2004, 306-312

[13] Steven N. Ward (2003). Classical Tsunami Theory-a la Ward

[14] Steven N.Ward. Tsunamis in The Encyclopedia of Physical Science and Technology, ed. R. A. Meyers, Academic Press, **Vol. 17**, 175-191

[15] Tatsuo Ohmachi et al. (2001). Simulation of Tsunami Induced by Dynamic displacement of Seabed due to Seismic Faulting, Bulletin of Seismological Society of America, **91:6**, 1898-1909